Electronic Supplementary Material (ESI) for New Journal of Chemistry.

Supplementary Information

Porous Graphene-$NiCo_2O_4$ Nanorod Hybrid Composite as High Performance Supercapacitor Electrode Material

Meenaketan Sethi[a], U Sandhya Shenoy[b], D Krishna Bhat[a]*

[a]Department of Chemistry, National Institute of Technology Karnataka, Surathkal, Mangalore-575025, India.

[b]Department of Chemistry, College of Engineering and Technology, Srinivas University, Mukka Mangalore - 574146, India.

*Corresponding author E-mail: denthajekb@gmail.com

Methods

Synthesis of GO: GO was prepared according to the improved Hummers method, reported elsewhere.[1,2] A calculated amount of graphite powder was stirred for 30 min with 9:1 mixture of H_2SO_4:H_3PO_4. This was followed by the slow addition of $KMnO_4$ in batches in order to avoid exothermic impact. The resultant mixture was heated at 50 °C for 12 h. The obtained dark brown suspension was poured into 200 mL ice cold water followed by the addition of 30% H_2O_2 till the effervesce ceases, changing the color of the suspension from dark brown to brilliant yellow color. The suspension was successively washed with deionized water, 30% HCl, ethanol and finally dried at 50 °C for 10 h to get GO powder.

Synthesis of PG: The synthesized GO powder (1 mg/mL) was dispersed in equal volume of ethylene glycol:water mixture and was ultrasonicated for 2 h in an ultrasonic bath. This exfoliated GO dispersion was taken in a stainless steel autoclave of 100 mL capacity and heated to 160 °C for 16 h. Later, the autoclave was cooled down to room temperature and the resultant products were repeatedly washed with deionized water followed by ethanol. The products were later dried in oven at 80 °C for 6 h to obtain PG.[2]

Electrochemical Measurements: The working electrodes were made by mixing the active material (5 PGNC - 30 PGNC), acetylene black and PVDF binder in a weight ratio of 8:1:1. Initially, active material and acetylene black were mechanically mixed together using a mortar and pestle and later a few drops of PVDF binder dissolved in NMP was added and mixed to get a slurry-like ink. The electrochemical properties of single electrode were evaluated by coating the above stated slurry like ink on a Ni sheet of 1×1 cm^2 area using Doctor's blade technique followed by drying and employing a 3-electrode method. The mass deposited on the sheet was

approximately 1 mg, as measured by a high precision Citizon analytical weighing balance with a readability of 0.0001 g. Here, the coated Ni sheet served as the working electrode, saturated calomel as reference electrode, and platinum wire as counter electrode, respectively.

For the supercapacitor device fabrication, the slurry-like ink was coated on one side of a Toray carbon paper of 2×2 cm^2 area using layer by layer brush coating technique. The coated carbon paper was heated at 60 °C for 8 h to reduce the effect of the binder used. The supercapacitor setup consisted of coated PG as working electrode material, 2 M KOH as an electrolyte, Whattman filter paper (same dimension as that of Toray carbon paper) soaked in the electrolyte as a separator and stainless-steel panels as current collectors. The mass deposited on single carbon paper was found to be approximately equal to 3 mg. The specific capacitance values from the CV and GCD curves were calculated according to the equation (1) and (2), respectively.

$$C_S = \frac{nA}{\Delta V \times m \times \nu} \qquad (1)$$

Where C_s = specific capacitance (F g^{-1}), A is the integrated area of the CV curve, ΔV is the maximum potential window (V), m is the deposited mass on one single electrode (g), and ν is the scan rate (V s^{-1}). A factor of n = 2 is multiplied owing to the formation of series capacitance in a 2-electrode cell, for 3-electrode system, n = 1.

$$C_s = n \times \frac{I \times \Delta t}{m \times \Delta V} \qquad (2)$$

Where C_s = specific capacitance (F g^{-1}), $\frac{I}{m}$ is the applied current density, Δt is the discharging time, ΔV is the maximum potential window to discharge the cell, n = 2 for 2-electrode system and n = 1 for 3-electrode system.

The energy density and power density of the prepared supercapacitor were calculated according to equation (3) and (4), respectively.

$$\text{Energy Density (Wh kg}^{-1}) = \frac{1}{2} C_s V^2 \times \frac{1000}{3600} \qquad (3)$$

$$\text{Power Density (W kg}^{-1}) = \frac{E}{t_d} \times 3600 \qquad (4)$$

Where, C_s = specific capacitance (F g^{-1}), V is the maximum potential window, E is the applied energy density, t_d is the discharging time.

The specific capacity (mAh g^{-1}) values were also calculated from the CV data according to the equation (5)

$$Q_s = \frac{1000 \times i \times t}{3600 \times m} \ (\text{mAhg}^{-1}) \qquad (5)$$

Where, (i/m) is the applied current density (1 A g^{-1}), and t is the discharge time.

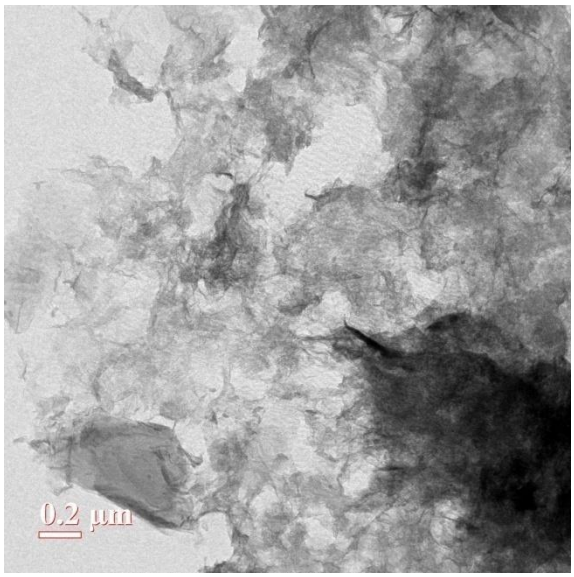

Figure S1. TEM image of PG.

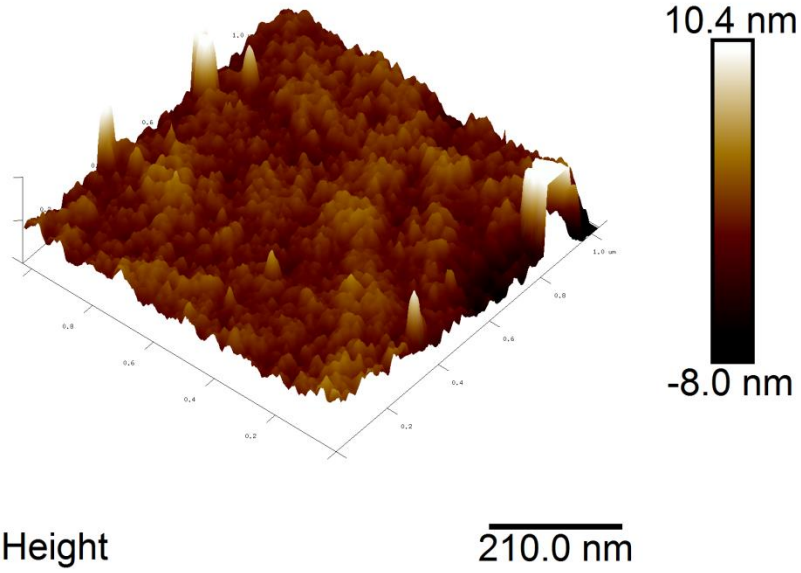

Figure S2. AFM image of PG.

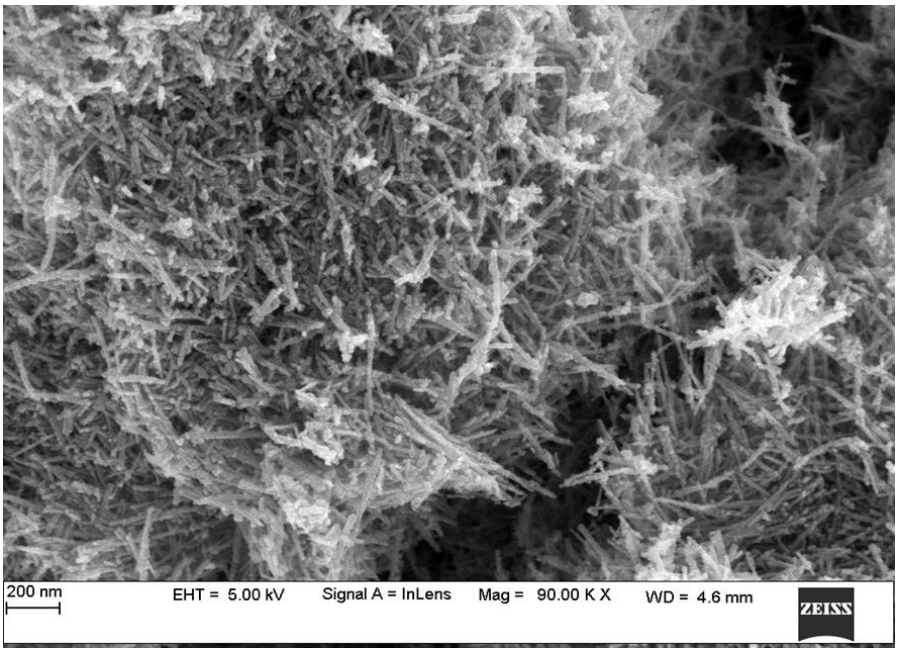

Figure S3. FESEM image of NC nanorods.

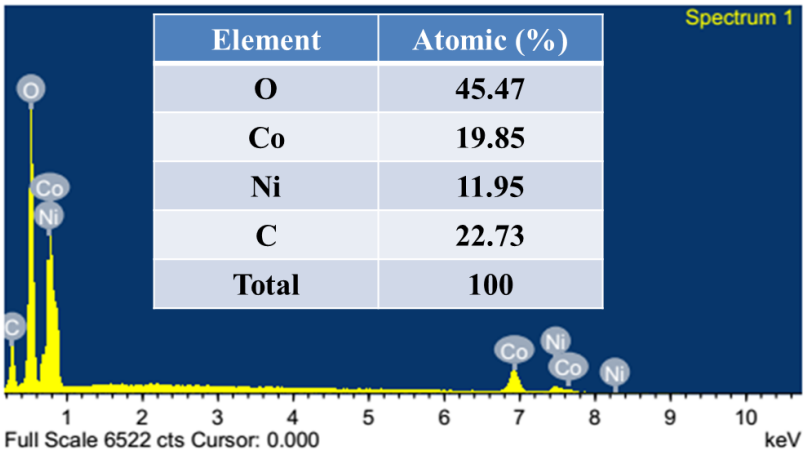

Figure S4. EDX profile of 10 PGNC with elemental data as inset.

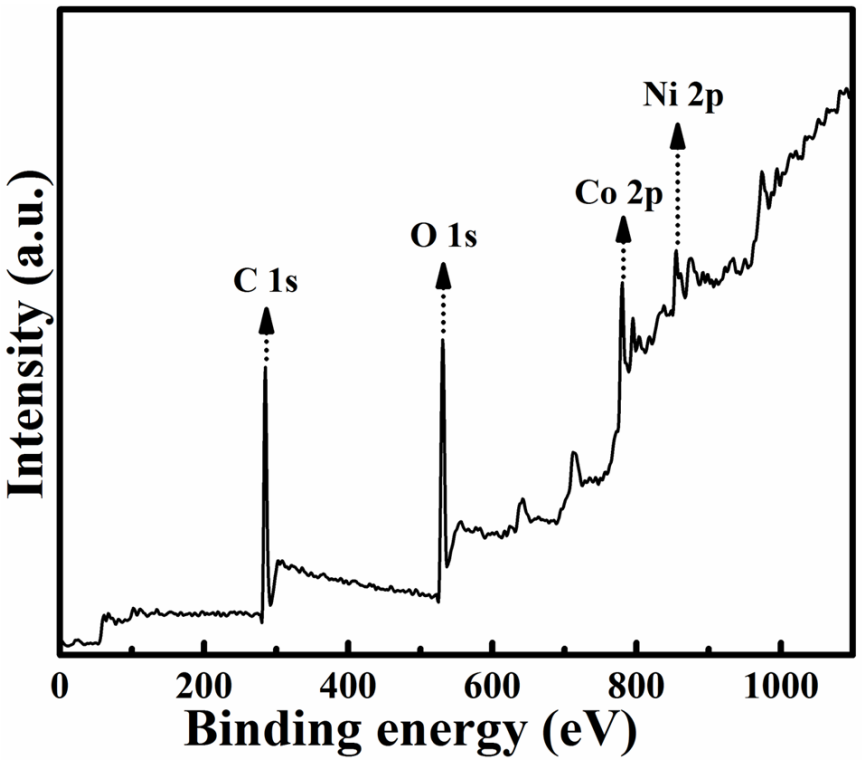

Figure S5. XPS survey spectrum of 10 PGNC.

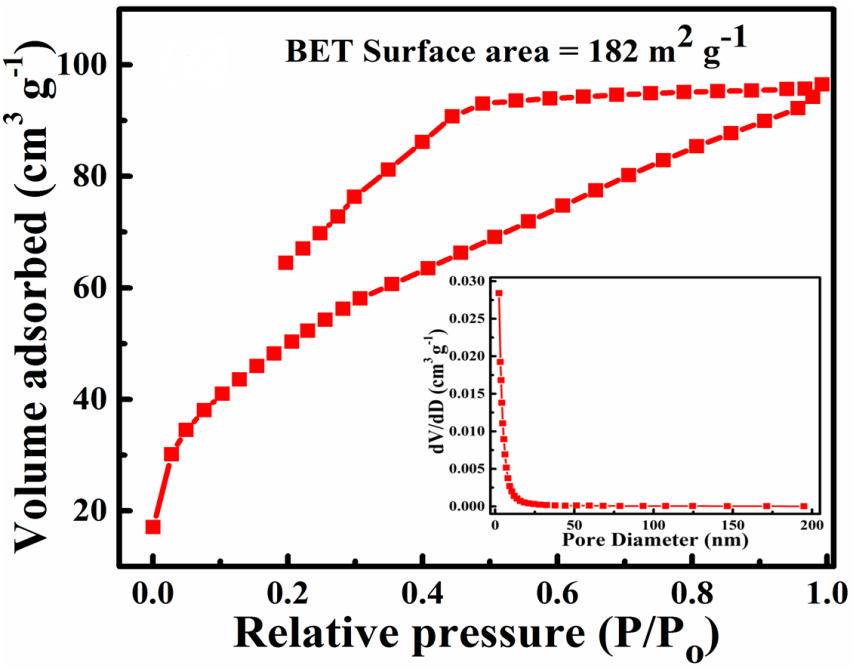

Figure S6. BET surface area of PG (inset shows the pore size distribution plot with mean pore diameter 3.2 nm).

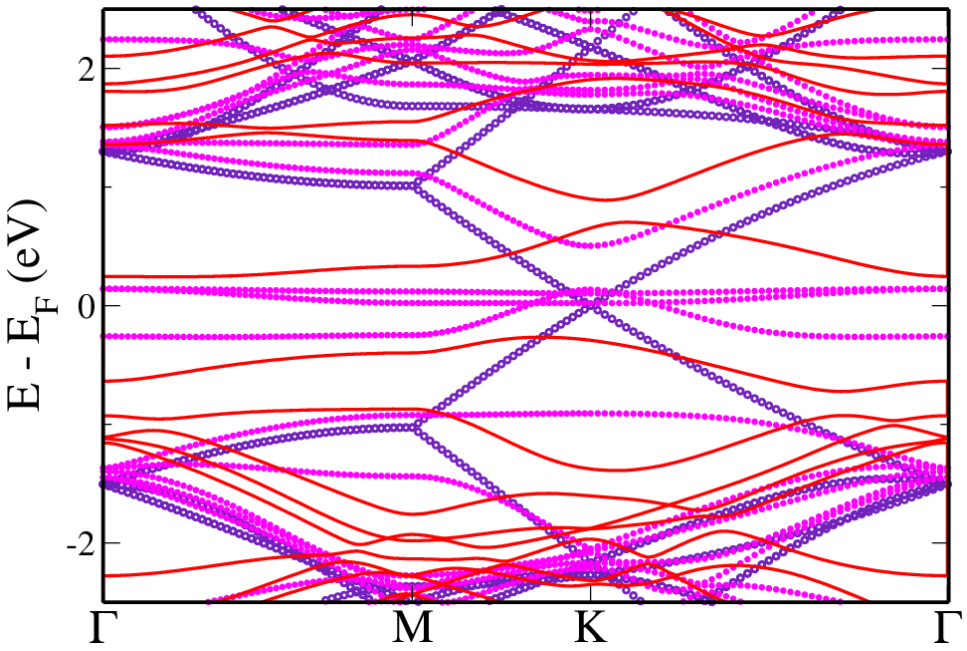

Figure S7. Electronic structure of defect free graphene (violet); PG with single C vacancy (magenta); PG with two C vacancies (red).

Table S1. PGNC composite samples and their corresponding specific capacity values.

PGNC composite	**Specific capacity (mAh g^{-1})**
5 PGNC	76.5
10 PGNC	210.5
15 PGNC	105.0
20 PGNC	92.8
25 PGNC	48.6
30 PGNC	20.0

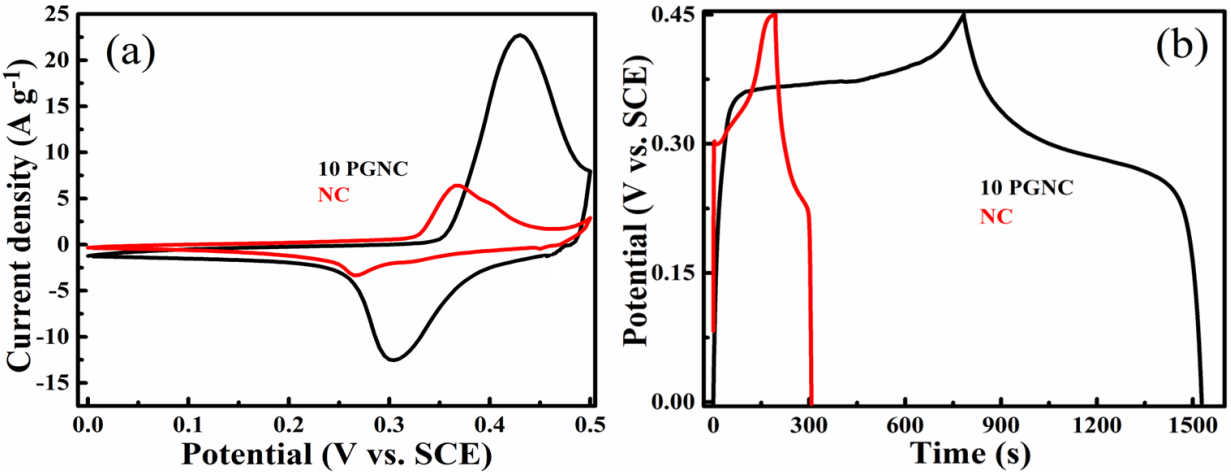

Figure S8. (a) CV curves at a constant scan rate of 5 mVs^{-1} and (b) GCD curves at a constant current density of 1 Ag^{-1}, of NC and 10 PGNC in a 3-electrode method.

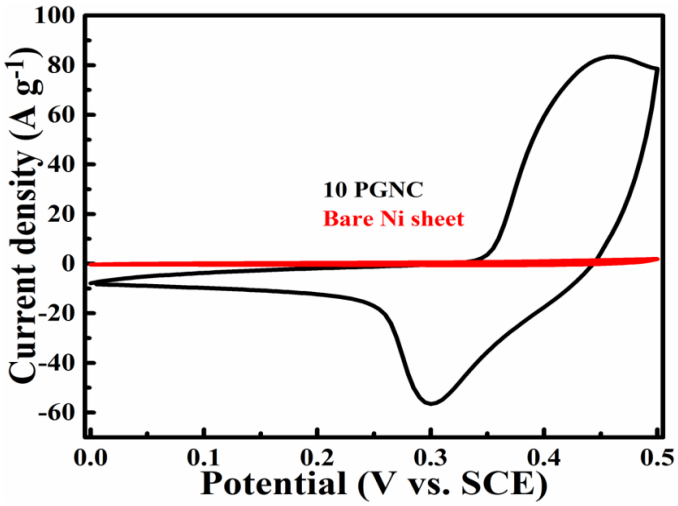

Figure S9. CV curves of bare Ni sheet and 10 PGNC at a constant scan rate of 50 mV s^{-1}.

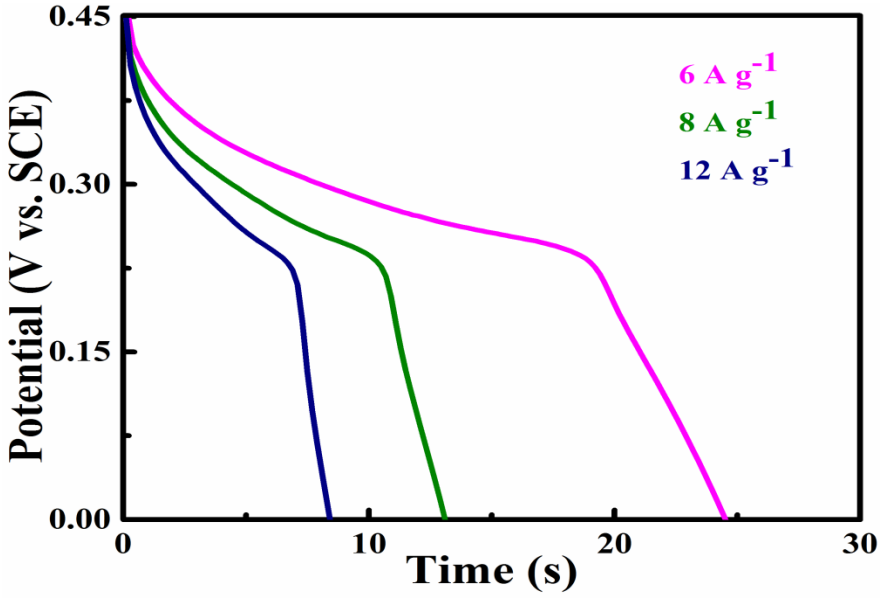

Figure S10. GCD curves of the 10 PGNC composite at current densities from 6-12 Ag^{-1}.

Table S2. Specific capacitance values of PGNC composites from CV data.

Composite	Scan rate (mV s^{-1})	Specific Capacitance (F g^{-1})
5 PGNC	5	735
	10	647
	20	589
	30	497
	50	382
15 PGNC	5	983
	10	874
	20	798
	30	627
	50	518
20 PGNC	5	942
	10	823
	20	736
	30	691
	50	593
25 PGNC	5	401
	10	382
	20	356
	30	312
	50	296
30 PGNC	5	264
	10	244
	20	233
	30	197
	50	159

Table S3. Specific capacitance values of PGNC composites from GCD data.

Composite	Current density (A g^{-1})	Specific Capacitance (F g^{-1})
5 PGNC	1	612
	2	397
	4	267
	6	198
	8	153
	12	107
15 PGNC	1	840
	2	485
	4	336
	6	267
	8	201
	12	145
20 PGNC	1	742
	2	683
	4	231
	6	187
	8	160
	12	157
25 PGNC	1	387
	2	290
	4	222
	6	186
	8	165
	12	141
30 PGNC	1	157
	2	141
	4	123
	6	110
	8	101
	12	90

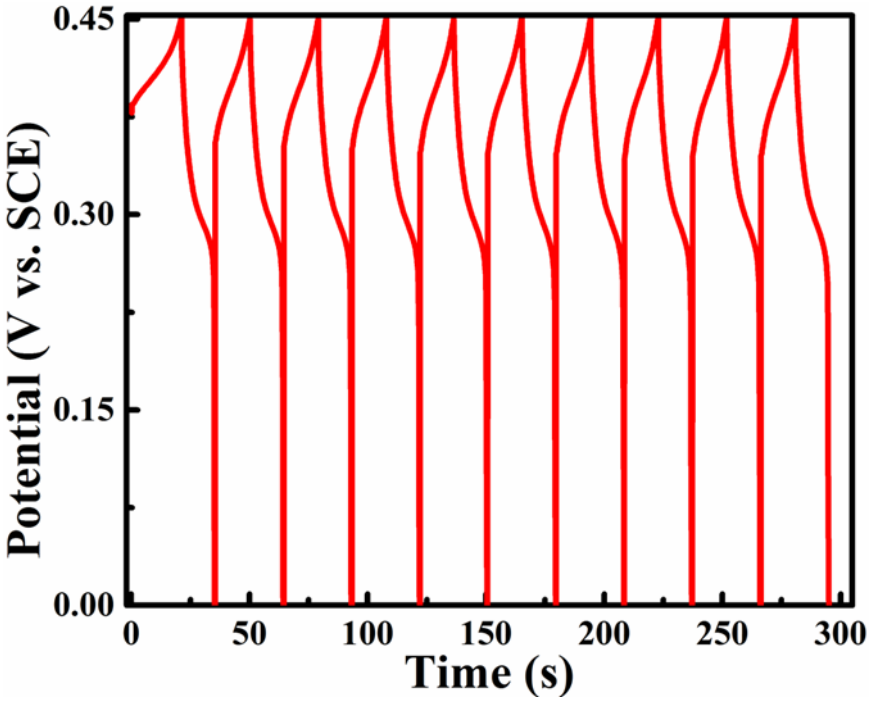

Figure S11. First 10 charge-discharge cycles for 10 PGNC electrode.

Table S4. Energy and power density of 10 PGNC electrode.

Current density (A g^{-1})	**Energy density (Whkg^{-1})**	**Power density (W kg^{-1})**
1	47.4	225.5
2	43.8	451.3
4	28.2	900.0
6	10.2	1353.8
8	7.8	1797.8
12	6.2	2704.2

Table S5. Comparison of electrochemical performance of 10 PGNC with literature.

Composites	Specific capacitance in 3 electrode system ($F\ g^{-1}$)	Stability	References
PGNC composite	1684 (1 A g^{-1})	94 %, 10000 cycles (8 A g^{-1})	Present work
3D mesoporous $NiCo_2O_4$@graphene	778 (1 A g^{-1})	90 %, 10000 cycles (10 A g^{-1})	Wei et al. 2014 (4)
$NiCo_2O_4$ nanoneedle/carbon cloth arrays	660 (2 A g^{-1})	91.8 %, 3000 cycles (2 A g^{-1})	Zhang et al. 2014 (5)
$NiCo_2O_4$ decorated dopamine derived carbon nanocomposites	667 (5 A g^{-1})	95%, 2000 cycles (10 A g^{-1})	Veeramani et al. 2016 (6)
rGO/ nickel cobaltite nanocomposites	613 (1 A g^{-1})	90.9 %, 2000 cycles (1 A g^{-1})	Foo et al. 2016 (7)
rGO- $NiCo_2O_4$ hollow spheres	971 (0.5 A g^{-1})	76 %, 5000 cycles (10 A g^{-1})	Mondal et al. 2017 (8)
rGO- porous $NiCo_2O_4$	1185 (2 A g^{-1})	98%, 10000 cycles (2 A g^{-1})	S. Al-Rubayeet al. 2017 (9)
$NiCo_2O_4$/rGO hybrid	932 (1 A g^{-1})	83.8 %, 5000 cycles(2 A g^{-1})	Jiang et al. 2018 (10)
$NiCo_2O_4$/CNF composite	786 (1 A g^{-1})	87 %, 5000 cycles (4 A g^{-1})	Yang et al. 2018 (11)
GO/MWCNT/$NiCo_2O_4$ hybrid composite	707 (2.5 A g^{-1})	88 %, 5000 cycles	Ramesh et al. 2018 (12)
rGO/ $NiCo_2O_4$ composite	1003 (1 A g^{-1})	57%, 10000 cycles (10 A g^{-1})	Zhang et al. 2019 (13)

$NiCo_2O_4$/Carbon composite	920 (1 A g^{-1})	94 %, 5000 cycles (1 A g^{-1})	Xu et al. 2019 (14)
Carbonized channels wrapped by $NiCo_2O_4$ nanosheets	1541 (1 A g^{-1})	85.8 %, 10000 cycles (10 A g^{-1})	Qu et al. 2019 (15)
$NiCo_2O_4$/NG composites	563 (1 A g^{-1})	90.5 %, 5000 cycles (3 A g^{-1})	Chang et al. 2019 (16)
rHGO/$NiCo_2O_4$@CF	1178 (1 A g^{-1})	87.4%, 5000 cycles (5 A g^{-1})	Li et al. 2019 (17)
N-doped porous carbon/$NiCo_2O_4$	948 (1 A g^{-1})	87.4%, 2000 cycles (10 A g^{-1})	Tang et al. 2019 (18)
SnO_2@$NiCo_2O_4$/N-MWCNTs	728(4 A g^{-1})	92.0 %, 5000 cycles (-)	Ramesh et al. 2019 (19)
FeCoNi@GNPs electrode material	538 (1 A g^{-1})	91.5 %, 5000 cycles(10 A g^{-1})	Li et al. 2019 (20)
$NiCo_2O_4$/3D-OPC electrode material	1297(0.5A g^{-1})	-	Dong et al. 2019 (21)

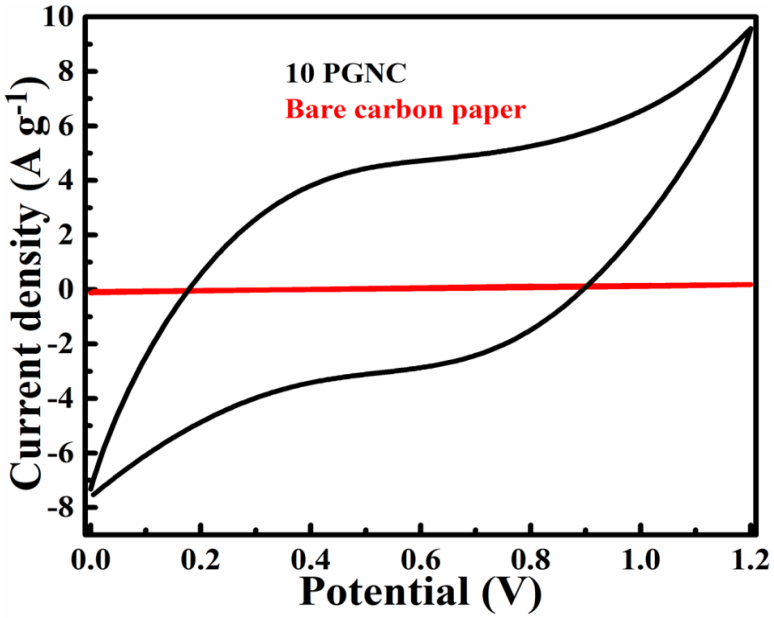

Figure S12. Electrochemical analysis of bare carbon paper and 10 PGNC composite in a fabricated supercapacitor device.

Table S6. Comparison of electrochemical performance of 10 PGNC in a symmetrical/ asymmetrical supercapacitor with reported literature.

Composites/material	Specific capacitance (F g^{-1}) in symmetrical supercapacitor cell	Specific capacitance (F g^{-1}) in asymmetrical supercapacitor cell	Stability	References
PGNC composite	266 @ 2 mV s^{-1} 225 @ 1 A g^{-1}	-	93 %, 10000 cycles (8 A g^{-1})	Present work
rHGO/$NiCo_2O_4$/CF and AC	-	192.5 @ 1 A g^{-1}	82.7 %, 5000 cycles (2 A g^{-1})	Li et al. 2019 (17)
$NiCo_2O_4$/3D-OPC//3D-OPC	-	82.2 @ 1 A g^{-1}	87.6 %, 3000 cycles (1 A g^{-1})	Dong et al. 2019 (21)
NCO/GA//AC	-	87 @ 1 A g^{-1}	78 %, 3000 cycles (1 A g^{-1})	Jiu et al. 2019 (22)
$NiCo_2O_4$/GQDs//AC	-	107 @ 1 A g^{-1}	71.8 %, 3000 cycles (4 A g^{-1})	Luo et al. 2019 (23)
$NiCo_2O_4$/3D N,S RGO	-	108 @ 2 A g^{-1}	125 %, 12000 cycles (10 A g^{-1})	Sivakumar et al. 2019 (24)
Co-Ni-OH/rGO/CC	151.46@ 2.5 A g^{-1}	-	85.65 %, 3000 cycles (5 A g^{-1})	Wang et al. 2019 (25)

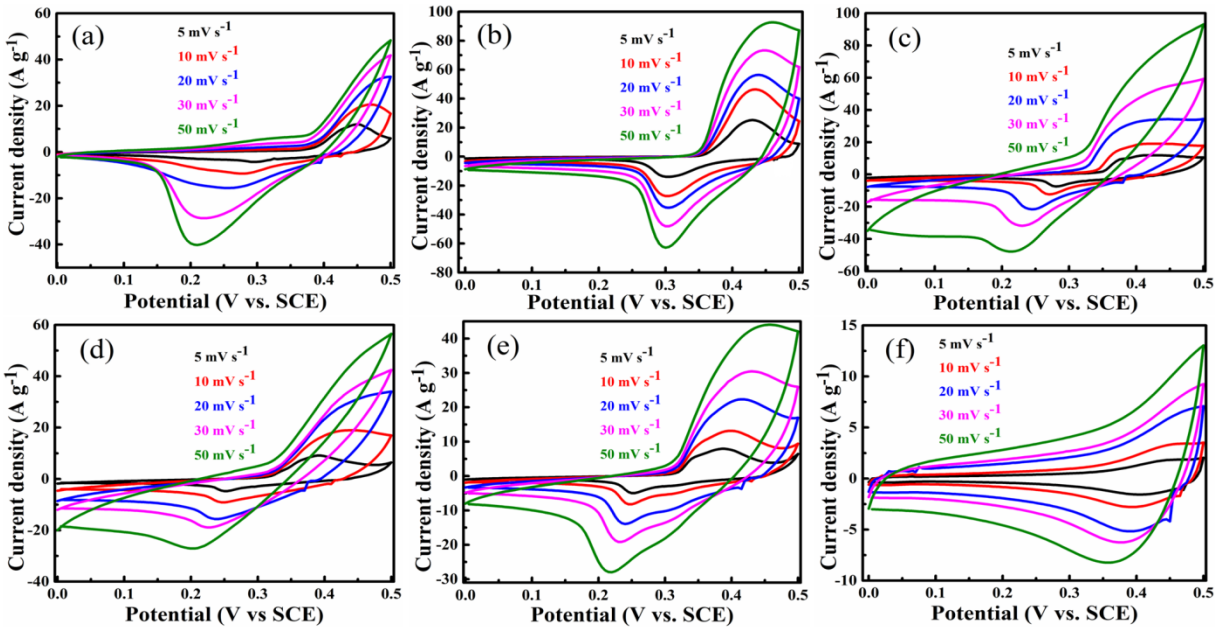

Figure S13. CV curves for (a) 5 PGNC, (b) 10 PGNC, (c) 15 PGNC, (d) 20 PGNC, (e) 25 PGNC and (f) 30 PGNC composite electrodes.

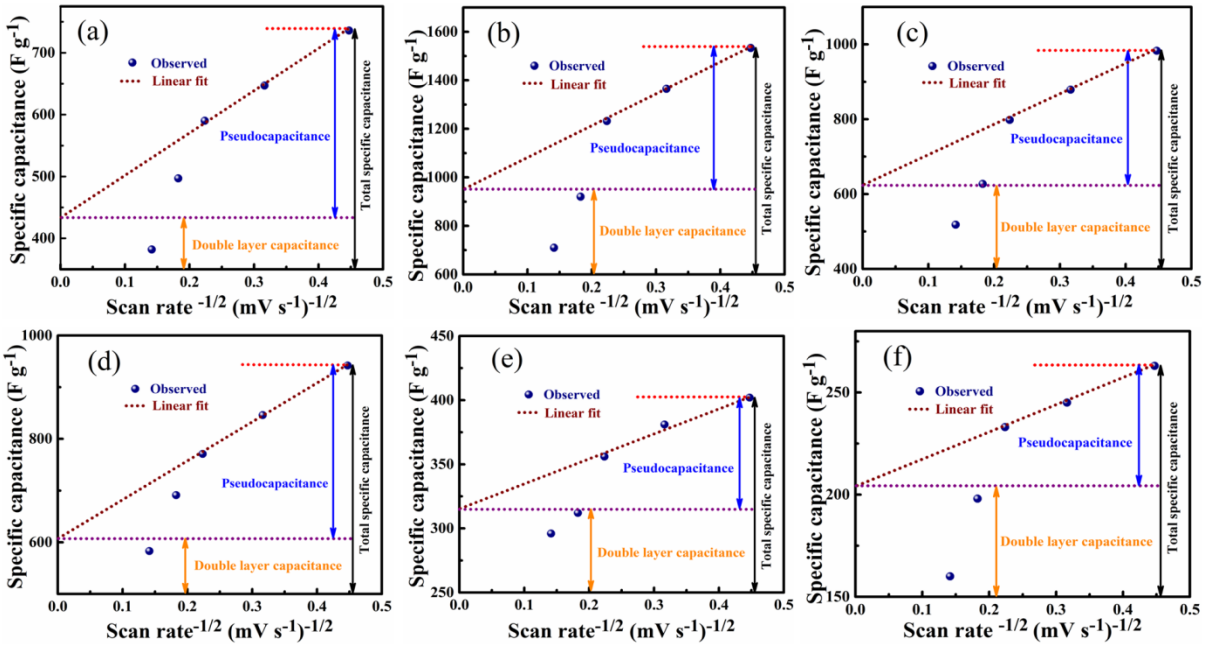

Figure S14. Graphical determination of capacitance contribution of (a) 5 PGNC, (b) 10 PGNC, (c) 15 PGNC, (d) 20 PGNC, (e) 25 PGNC and (f) 30 PGNC composite electrodes.

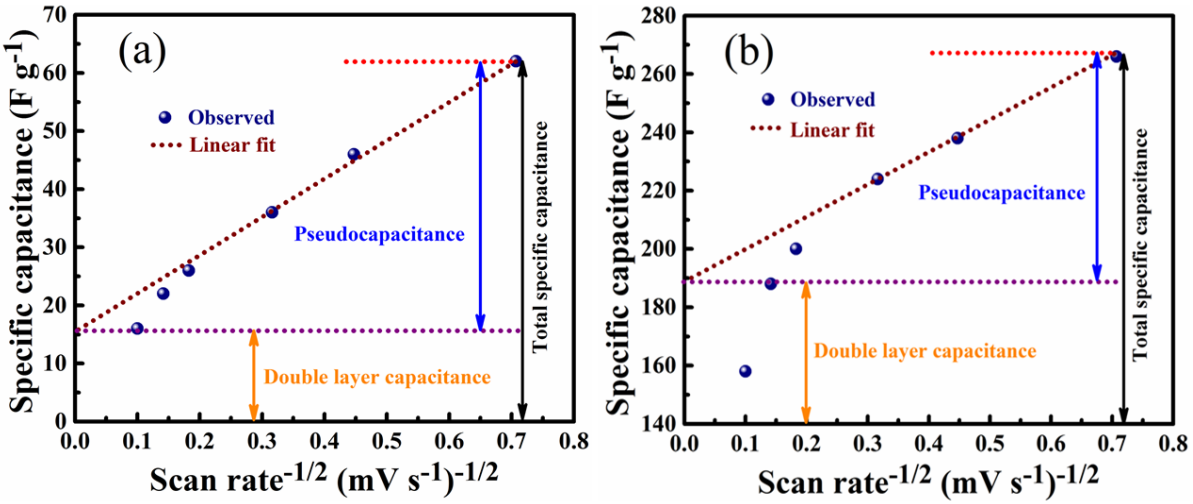

Figure S15. Graphical determination of capacitance contribution of (a) NC and (b) 10 PGNC composite fabricated supercapacitor.

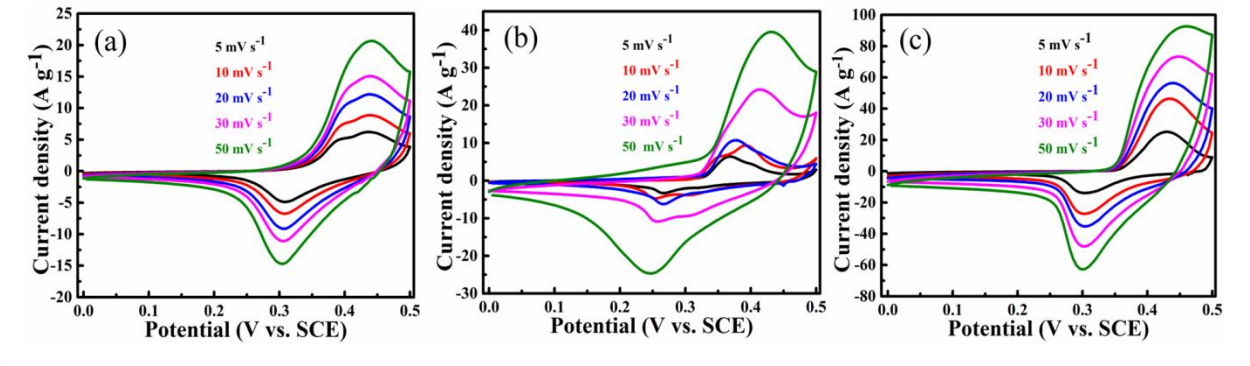

Figure S16. CV curves of (a) PG, (b) NC and (c) 10 PGNC composite electrodes.

References

1 M.M.J. Sadiq, U. S. Shenoy and D.K. Bhat, *RSC Adv.*, 2016, **6**, 61821−61829.

2 M. Sethi, H. Bantawal, S. U. Shenoy and D.K. Bhat, *J. Alloys Compd.*, 2019, **799**, 256−266.

3 S. Chen, M. Mao, X. Liu, S. Hong, Z. Lu, S. Sang, K. Liu and H. Liu, *J. Mater. Chem. A*, 2016, **4**, 4877−4881.

4 Y. Wei, S. Chen, D. Su, B. Sun, J. Zhu and G. Wang, *J. Mater. Chem. A*, 2014, **2**, 8103−8109.

5 D. Zhang, H. Yan, Y. Lu, K. Qiu, C. Wang, C. Tang, Y. Zhang, C. Cheng and Y. Luo, *Nanoscale Res. Lett.*, 2014, **9**, 139.

6 V. Veeramani, R. Madhu, S.M. Chen, M. Sivakumar, *ACS Sustainable Chem. Eng.*, 2016, **4**, 5013−5020.

7 C.Y. Foo, H.N. Lim, M.A.B. Mahdi, K.F. Chong, N. M. Huang, *J. Phys. Chem. C*, 2016, **120**, 21202−21210.

8 A. Mondal, S. Maiti, S. Mahanty and A.B. Panda, *J. Mater. Chem.A*, 2017, **5**, 16854−16864.

9 S. Al-Rubaye, R. Rajagopalan, S. X. Dou and Z. Cheng, *J. Mater. Chem. A*, 2017, **5**, 18989−18997.

10 H. Jiang, K. Yang, P. Ye, Q. Huang, L. Wang and S. Li, *RSC Adv.*, 2018, **8**, 37550−37556.

11 Y. Yang, D. Zeng, L.Gu, B. Liu, F. Guo, Y. Ren and S. Hao, *Electrochim. Acta*, 2018, **286**, 1−13.

12 S. Ramesh, D. Vikraman, H.S. Kim, H.S. Kim and J.H. Kim, *J. Alloys Compd.*, 2018, **765**, 369−379.

13 S. Zhang, H. Gao, J. Zhou, F. Jiang and Z. Zhang, *J. Alloys Compd.*, 2019, **792**, 474−480.

14 Z. Xu, L. Yang, Q. Jin and Z. Hu, *Electrochim. Acta*, 2019, **295**, 376−383.

15 Z. Qu, M. Shi, H. Wu, Y. Liu, J. Jiang and C. Yan, *J. Power Sources*, 2019, **410**,179−187.

16 X. Chang, W. Li, Y.Liu, M. He, X. Zheng, X. Lvand Z. Ren, *J. Alloys Compd.*, 2019, **784** 293−300.

17 S. Li, K. Yang, P. Ye, H. Jiang, Z. Zhang, Q. Huang and L. Wang, *Appl. Surf. Sci.*, 2019, **473**, 326−333.

18 Q. Tang, Y. Zhou, L. Ma and M. Gan, *J. Solid State Chem.*, 2019, **269**, 175−183.

19 S. Ramesh, D. Vikraman, K. Karuppasamy, H.M. Yadav, A. Sivasamy, H.S. Kim, J. H. Kim and H.S. Kim, *J. Alloys Compd.*, 2019, **794**, 186−194.

20 Y. Li, J. Zhai, L. Zhao, J. Chen, X. Shang, C. Song, J. Chen, S. Liu and F. Meng, *J. Solid State Chem.*,2019, **276**,19−29.

21 K. Dong, Z. Wang, M. Sun, D. Wang, S. Luo and Y. Liu, *J. Alloys Compd.*, 2019, **783**, 1−9.

22 H. Jiu, L. Jiang, Y. Gao, Q. Zhang and L. Zhang, *Ionics*, 2019, 1−7.

23 J. Luo, J. Wang, S. Liu, W. Wu, T. Jia, Z. Yang, S. Mu and Y. Huang, Carbon, 2019, **146**,1−8.

24 P. Sivakumar, M. Jana, M. Kota, H. S. Lee and H.S. Park, *J. Alloys Compd.*, 2019, **781**, 515−523.

25 D. Wang, A. Wei, L. Tian, A. Mensah, D. Li, Y. Xu and Q. Wei, *Appl. Surf. Sci.*, 2019, **483**, 593−600.